Journal of Applied Mechanics and Technical Physics, Vol. 45, No. 4, pp. 466–476, 2004

REACHING HIGH TEMPERATURES BY COMPRESSING A VAPOR BUBBLE

P. I. Mel'nikov, V. G. Makarenko, and M. G. Makarenko

UDC 533.2+534.2

The process of compression of a vapor bubble under the action of an instantaneously applied pressure is considered. The effect of initial parameters on compression dynamics is analyzed. Conditions of emergence of a shock wave inside the bubble are considered. It is shown that the temperature in the bubble is lower than 10^4 K *under uniform compression.*

Key words: *vapor bubble, compression, high temperature, shock wave.*

Introduction. Compression of a gas bubble involves the effect of sonoluminescence [1–3] associated with reaching high temperatures: above 10^4 K [4, 5]. Calculations supporting the possibility of reaching such temperatures were performed for an inert gas compressed in water [6, 7]; ionization and the influence of evaporated vapor were ignored. Taleyarkhan et al. [8] observed the emergence of neutrons due to bubble cavitation, which indicates that the temperatures are even higher (above $5 \cdot 10^6$ K). The explanation of this effect is related to condensation of a significant part of vapors onto the bubble walls and formation of a shock wave [8].

The most complicated problem in studying cavitation of a vapor bubble is the interaction between the vapor and the water surface. This interaction is considered on the basis of the Hertz–Knudsen–Langmuir formula [9, 10] with an accommodation coefficient varied within 0.006–1 [11]. With such a scatter, the accommodation coefficient is used either as a free parameter [8] or as a fitting parameters for a particular experiment [12]. The accommodation coefficient depends not only on the temperature of the water surface but also, possibly, on the vapor flux [11, 13]. The coefficient obtained by fitting an experiment has an integral character and can be used only for estimates in situations close to this experiment [12].

Another difficulty in cavitation calculations is associated with the allowance for the change in the state of the substance. Many authors use a simplified approach, choosing an inert gas as a compressed substance [5, 6] or applying the equations for a gas with a constant heat capacity to describe the state of the vapor [12]. In calculating the compression dynamics of a vapor bubble, Akhatov et al. [12] accurately took into account almost all possible effects, even insignificant ones, such as the temperature jump and transferred momentum at the interface between the media. Nevertheless, the vapor was considered in a simplified formulation, as a Van-der-Waals gas with the ratio of specific heats equal to 1.3. Taking into account the change in the state of water vapors (increase in heat capacity and dissociation) will reduce the final calculated temperature severalfold (depending on the degree of compression). The change in the state of water vapors was taken into account in [14, 15] in connection with detonation processes inside the bubble. In these works, the thermodynamic parameters of the gas were calculated by the "approximate kinetic model" developed in [16–18]. We calculated the state of vapor in accordance with the law of mass action [19] with allowance for rapid compression kinetics.

In the present work, we consider the compression of a vapor bubble under the action of an instantaneously applied pressure. The compression process is analyzed to find the conditions of reaching high temperatures at the final stage of compression.

Joint-Stock Company "Katalizator," Novosibirsk 630058. Translated from Prikladnaya Mekhanika i Tekhnicheskaya Fizika, Vol. 45, No. 4, pp. 13–25, July–August, 2004. Original article submitted January 27, 2003; revision submitted March 29, 2003.

1. Model of Compression of a Vapor Bubble. An analysis of the works on accommodation-coefficient measurements [13, 20] shows that the latteris high in experiments with a rapid change in the surface layer of water [21–23], which is typical of cavitation of the vapor bubble. Assuming that the accommodation coefficient is of the order of unity, we calculate the bubble-compression dynamics for the case with the maximum possible final temperature. Such an approach allows us to reveal conditions at which the most intense heating is reached. If the accommodation coefficient is high, the equilibrium calculation and the calculation by the Hertz–Knudsen–Langmuir equation are little different [11]. In our analysis, we used the condition of equilibrium at the vapor–liquid interface [24].

If the bubble is compressed with a subsonic velocity, the pressure inside the bubble is uniform. The calculations show that the pressures at the center of the bubble and its periphery differ by no more than 20% when the bubble boundary reaches half of the velocity of sound. The temperature is higher at the center of the bubble. If the compression is rather fast, the temperature inside the bubble is close to uniform and drastically decreases near the boundary [12]. Most vapor particles have a close temperature if the temperature-drop layer thickness is much smaller than the bubble radius ($d_T \ll R$, this ratio was maintained in the calculations). The estimates show that thermal conductivity has a weak effect on compression parameters.

The pressure near the bubble boundary and, hence, at its center is equilibrium and is determined by the temperature on the water surface. During bubble compression, the equilibrium pressure is sustained due to vapor condensation at the vapor–liquid interface. This leads to water heating and, as a consequence, to an increase in pressure inside the bubble. When the boundary layer reaches the critical temperature $T_{\rm cr} = 647.28$ K, condensation is terminated, and the pressure inside the bubble is no longer equilibrium. The vapor–liquid interface disappears, but the density difference remains. This dense spherical piston will continue to compress the vapor inside the bubble. We assume that the further compression of the vapor will occur in the same manner as for a gas not interacting with water. The compression process can be divided into two phases: vapor phase and gas phase (after reaching the critical temperature $T_{\rm cr}$ at the boundary).

2. Bubble Compression in the Vapor Phase. We write the heat-conduction equation for water near the vapor–liquid interface:

$$\frac{\partial T}{\partial t} + v\,\frac{\partial T}{\partial r} = æ\,\frac{1}{r^2}\,\frac{\partial}{\partial r}\,r^2\,\frac{\partial T}{\partial r}.$$

Here, t is the time, r is the radial coordinate, v is the velocity, and æ is the thermal diffusivity. We replace $x = r^3 - R^3$ (R is the bubble radius). Taking into account that $v = \dot{R}(R/r)^2$, we obtain

$$\frac{\partial T}{\partial t} = 9æ\,\frac{\partial}{\partial x}\,(R^3 + x)^{4/3}\,\frac{\partial T}{\partial x}. \qquad (1)$$

With allowance for the relation $\partial T/\partial t \gg 12æR\partial T/\partial x$, which is valid for all parameters we consider, we simplify Eq. (1):

$$\frac{\partial T}{\partial u} = 9æ\Big(1 + \frac{x}{R^3}\Big)^{4/3}\,\frac{\partial^2 T}{\partial x^2}. \qquad (2)$$

Here $u = \int\limits_0^t R(\tau)^4\,d\tau$. Assuming that the temperature at the beginning of compression is T_0 in the entire space, we write the solution of Eq. (2) near the interface ($x \ll R^3$) in the form

$$T(x,t) = T_0 + \frac{x}{6\sqrt{\pi æ}}\int\limits_0^u \frac{T_R(\tau) - T_0}{(u-\tau)^{3/2}}\,\exp\Big(-\frac{x^2}{36æ(u-\tau)}\Big)\,d\tau,$$

where T_R is the temperature at the interface. Then, the heat flux at the interface is

$$-\frac{\lambda}{k}\,\frac{\partial T}{\partial r} = \frac{C_p\rho_w}{k}\,R^2\sqrt{\frac{æ}{\pi}}\int\limits_0^u \frac{\dot{T}_R(\tau)}{\sqrt{u-\tau}}\,d\tau. \qquad (3)$$

Here λ is the thermal conductivity, $C_p\rho_w$ is the volume heat capacity of water, and k is the Boltzmann constant; the temperature T is expressed in energy units.

The heat flux due to vapor condensation is

$$q = -\frac{H(T_R) + E(T) - E(T_R)}{4\pi R^2}\,\frac{dN}{dt} = -\frac{H(T_R) + E(T) - E(T_R)}{4\pi R^2}\,\frac{d}{dt}\,\frac{PV}{T},$$

where N is the number of vapor molecules in the bubble, P, V, and T are the parameters of vapor in the bubble, $E(T)$ is the total energy of the water molecule, and H is the vapor-formation heat. Comparing this heat flux with the heat flux (3), we obtain the equality

$$4\,\frac{C_p\rho_w}{k}\,\sqrt{\pi\text{\ae}}\int\limits_0^u \frac{\dot{T}_R(\tau)}{\sqrt{u-\tau}}\,d\tau + (H(T_R) + E(T) - E(T_R))\,\frac{d}{du}\,\frac{P(T_R)V}{T} = 0. \tag{4}$$

This equation implies that the condensation heat H and the equilibrium pressure of vapor P depend only on the temperature at the interface T_R. The dynamics of volume variation is determined by the Herring–Gilmore equation [25]

$$R\,\frac{d^2R}{dt^2} + \frac{3}{2}\Big(\frac{dR}{dt}\Big)^2 = \frac{P_s - P_w}{\rho_w} + \frac{R}{\rho_w c_w}\frac{dP_s}{dt}, \qquad P_s = P(T_R) - \frac{2\sigma}{R} - 4\mu\,\frac{dR}{R\,dt}. \tag{5}$$

Here R is the current radius of the bubble, P_s is the pressure in water near the bubble boundary, $P(T_R)$ is the gas pressure in the bubble, P_w is the pressure in water at infinity, σ is the surface tension of water, μ is the viscosity of water, and c_w is the velocity of sound in water.

Thermal conductivity being neglected, the change in energy of the vapor bubble $d\,NE$ is determined by the energy loss due to the decrease in the number of molecules $E\,dN$ and the work on bubble compression $P\,dV$:

$$d\,NE = E\,dN - P\,dV. \tag{6}$$

After the replacements $dE = C\,dT$ and $PV = NT$, we obtain

$$C\,\frac{dT}{T} + \frac{dV}{V} = 0. \tag{7}$$

For $C = \text{const}$, we have the conventional adiabat $TV^{1/C} = \text{const}$. Note, the adiabat expressed in terms of pressure relates three quantities $PV^{1+1/C}/N = \text{const}$.

The dependence of saturated vapor pressure on temperature can be found, e.g., in [26]. The heat capacity is determined by the formulas of [19] and the data of [27]:

$$C = 3 + \Big(\frac{0.198}{2T\sinh\,(0,198/2T)}\Big)^2 + \Big(\frac{0.454}{2T\sinh\,(0.454/2T)}\Big)^2 + \Big(\frac{0.466}{2T\sinh\,(0.466/2T)}\Big)^2 \tag{8}$$

(hereinafter, the temperature is expressed in electron-volts). Combining relations (4), (5), and (7), making the obvious substitution $V = 4\pi R^3/3$, and nondimensionalizing the parameters $z = R/R_0$ and $\xi = u/(\tau_0 R_0^4)$, where R_0 is the initial radius and $\tau_0 = 0.915 R_0\sqrt{\rho_w/P_w}$ is the time of the vacuum-bubble collapse, we obtain

$$3\,\frac{C_p\rho_w}{kR_0}\sqrt{\frac{\text{\ae}\tau_0}{\pi}}\int\limits_0^\xi \frac{\dot{T}_R(\tau)}{\sqrt{\xi-\tau}}\,d\tau + (H(T_R) + E(T) - E(T_R))\,\frac{P(T_R)z^3}{T}\Big(\frac{dP(T_R)}{P(T_R)\,d\xi} + 3\Big(1 + \frac{1}{C}\Big)\frac{dz}{z\,d\xi}\Big) = 0,$$

$$C\,\frac{dT}{T} + 3\,\frac{dz}{z} = 0, \tag{9}$$

$$z\,\frac{d^2z}{d\xi^2} + 5.5\Big[\frac{dz}{d\xi}\Big]^2 = 0.915^2 z^{-8}\Big(\frac{P_s}{P_w} - 1\Big) + 0.915\,\frac{z^{-3}}{c_w}\sqrt{\frac{P_w}{\rho_w}}\,\frac{dP_s}{P_w\,d\xi}.$$

The solution of system (9) is determined by three parameters: initial radius R_0, compression pressure P_w, and initial temperature T_0. If the initial pressure in the bubble is low ($P_0 \ll P_w$), the vapor pressure affects the dynamics of radius variation only at the final stage of compression. Hence, neglecting P_s in the third equation of system (9), we find that the relative bubble radius z is almost independent of the initial parameters. The temperature in the bubble is determined by the initial temperature and relative radius of the bubble: $T(T_0, z)$. In the first equation of (9), the initial parameters enter only the coefficient at the integral in the form $R_0\sqrt{P_w}$. Hence, if the water and vapor temperature are identical in the beginning of compression, the temperature at the interface can be written

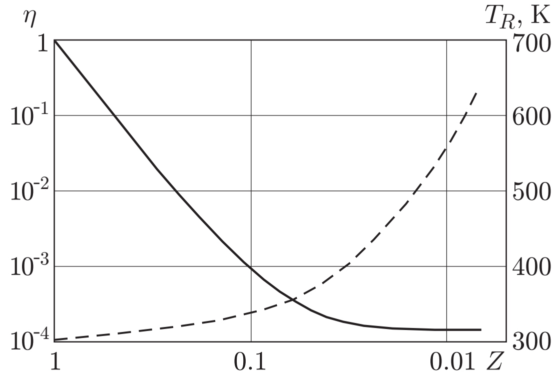

Fig. 1. Relative mass of vapor (solid curve) and temperature at the interface (dashed curve) for $P_w = 5$ bar, $R_0 = 1$ mm, and $T_0 = 30$°C.

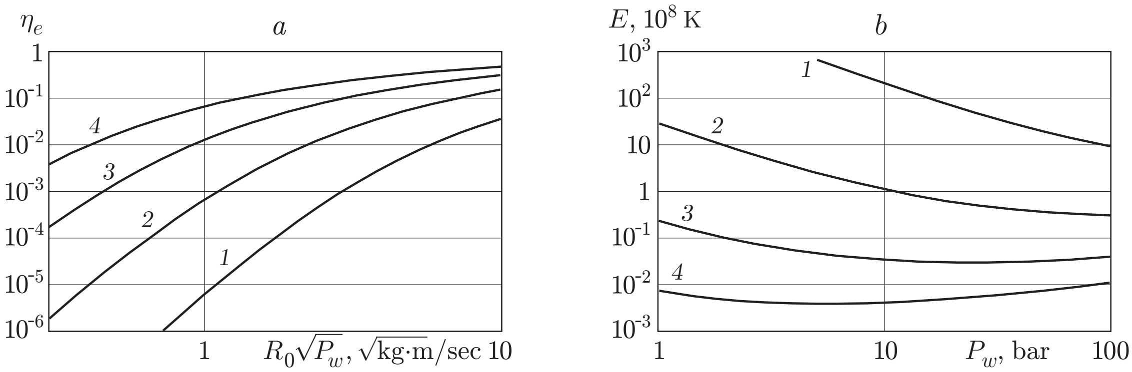

Fig. 2. Residual relative mass of vapor (a) and expected energy of vapor (b) for $R_0 = 1$ mm: $T_0 = 20$ (1), 30 (2), 40 (3), and 50°C (4).

as a function of two parameters and a variable quantity z: $T_R(R_0\sqrt{P_w}, T_0, z)$. Thus, the parameters R_0 and P_w determine the dynamics of bubble parameters until the final stage of compression (when the influence of the gas pressure P_s becomes noticeable) only in the combination $R_0\sqrt{P_w}$.

The most important quantity at the final stage of compression is the mass of the remaining vapor. We determine the relative mass of vapor $\eta = M/M_0$ (M and M_0 are the current and initial masses of vapor in the bubble) and follow its dependence on z (Fig. 1). When the rate of the bubble-radius decrease becomes high, the vapor mass is stabilized. The mass exchange with the bubble surface is almost terminated even before the critical temperature equal to 647.28 K is reached at the boundary, i.e., the transition to the gaseous regime of compression is smooth.

The relative mass of the vapor at the end of compression η_e depends only on two parameters T_0 and $R_0\sqrt{P_w}$ (see above). As is seen from Fig. 2, η_e rapidly decreases with decreasing $R_0\sqrt{P_w}$. An increase in the temperature T_0 leads to a strong increase in the initial pressure P_0 and, as a consequence, to an increase in η_e. The final relative mass of vapor η_e can reach very low values.

Compression of the vapor bubble was calculated for a pure vapor (without any admixtures). The other substance evaporated from water (e.g., air) should behave as a gas not interacting with the water surface. In the case of strong condensation of vapor, this substance can become the dominating one rather than a small additive, which should be taken into account in calculating the final stage of bubble compression.

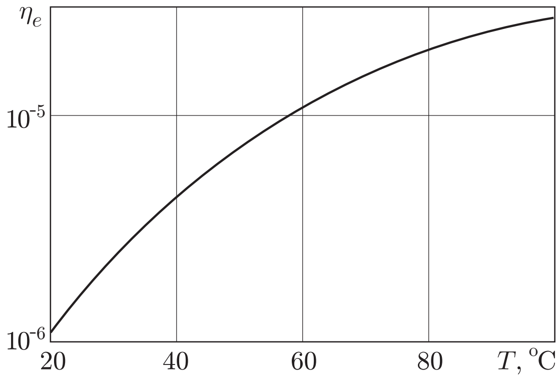

Fig. 3. Minimum relative mass of the vapor versus the initial temperature.

A strong decrease in the amount of the compressed substance can lead to a significant increase in the final temperature. The energy of the vapor molecule at the end of compression is expected to be

$$E = \frac{P_w V_0}{N} = \frac{P_w}{P_0} \frac{T_0}{\eta_e(R_0\sqrt{P_w}, T_0)}. \tag{10}$$

Here V_0 is the initial volume of the bubble. This energy coincides with the real value in the case of small losses on acoustic radiation and heating of water at the bubble boundary. The value determined by formula (10) is the estimate from above for the total energy per one water molecule at the end of compression. The higher the expected energy, the higher the maximum reachable temperature in the bubble. For a fixed R_0, the energy E with increasing pressure P_w first decreases, reaching a minimum as η_e approaches unity, and then increases (see Fig. 2b).

Because of vapor condensation, the mean free path l can become smaller than the bubble radius, and a complete collapse of the cavity can occur. We introduce the parameter $s = l/R$ and trace its dependence on z. As a criterion of the complete collapse, we use the condition $s_{\max} > 1$. An analysis of the dependence $s(z)$ shows that it reaches the maximum at the point where the dependence $\eta(z)$ starts to stabilize (see Fig. 1) and then decreases again with decreasing z. The boundary of the complete collapse mode is assumed to be the equality $s(z) = 1$ at this "critical" point. Numerical calculations in a wide range of initial parameters yielded the parametric relation

$$P_0 R_*^{0.7} P_w^{1/4} = 0.0334, \tag{11}$$

which corresponds to the boundary of the complete collapse mode (hereinafter, P is measured in bars and R is measured in millimeters; R_* is the radius corresponding to the boundary of the complete collapse). Note also that relation (11) is also the boundary for the accepted model of temperature distribution (see Sec. 1). The condition of smallness of the temperature-drop layer thickness $d_T \ll R$ is violated when the mean free path becomes greater than the bubble radius. The complete collapse will occur at $R_0 < R_*$. For fixed P_0 and P_w, a small change in the initial radius R_0 relative to R_* yields a significant change in the parameter s at the critical point. Therefore, even for $R_0 \gtrsim R_*$, the complete collapse is not reached. It is for these values of R_0 that the minimum (but not zero) amount of the residual gas and, hence, the highest value of the final temperature will be reached. Two initial parameters being fixed, we can find, using Eq. (11), the third parameter for which the amount of vapor at the final stage of the collapse is minimum. Figure 3 shows the dependence of the minimum reachable value of η_e on the initial temperature T_0 for $P_w = 10$ bar.

Substituting R_* from Eq. (11) into the formula for the energy of the water molecule (10), we obtain the maximum possible energy for fixed P_0 and P_w. A numerical analysis shows that this quantity is approximately described by the formula

$$E^{\max} = 3 \cdot 10^7 P_w^{1/4} P_0^{-2}.$$

The energy here is expressed in Kelvin. According to this formula, the expected temperature at the end of compression can reach tremendous values. However, this requires a soft compression mode without formation of shock waves.

A temperature for which dissociation should be taken into account is reached in the course of compression.

3. Chemically Equilibrium Composition of Water Vapor. To describe the water-vapor composition, we introduce the relative pressures $p_i = P_i/P$, where P_i is the partial pressure of the ith gas and $P = \sum_i P_i$ is the total pressure of the gas. In chemical equilibrium, according to the law of mass action, we obtain the following relation for the process of molecular dissociation $ab \to a + b$:

$$\frac{p_a p_b}{p_{ab}} = \frac{g_a g_b}{g_{ab}} \frac{Z_a(T) Z_b(T)}{Z_{ab}(T)} \Big(\frac{\mu_{ab}}{2\pi\hbar^2}\Big)^{3/2} \frac{T^{5/2}}{P} \exp\Big(-\frac{D_{ab}}{T}\Big). \tag{12}$$

Here, g_i is the statistical weight of the electron term of the ith species, $\mu_{ab} = m_a m_b/(m_a + m_b)$ is the reduced mass, $Z_i(T)$ is the statistical sum of rotational and vibrational degrees of freedom, D_{ab} is the dissociation potential, and T is the vapor-mixture temperature expressed in energy units. Water vapors consist of six species: four molecules and two atoms: H_2O, H_2, O_2, OH, H, and O. Four relations (12) and two relations of particle balance

$$p_{\mathrm{H_2O}} + p_{\mathrm{H_2}} + p_{\mathrm{O_2}} + p_{\mathrm{OH}} + p_{\mathrm{H}} + p_{\mathrm{O}} = 1,$$

$$2(p_{\mathrm{H_2O}} + 2p_{\mathrm{O_2}} + p_{\mathrm{OH}} + p_{\mathrm{O}}) = 2p_{\mathrm{H_2O}} + 2p_{\mathrm{H_2}} + p_{\mathrm{OH}} + p_{\mathrm{H}}$$

make it possible to determine all quantities $p_i(T, P)$ for known dependences $Z_i(T)$ (it is assumed that the ratio between the hydrogen and oxygen nuclei in the vapor mixture is always 2 : 1, as in the water molecule).

The statistical weights of the atoms (see [28]) are expressed via the spin and the total moment of the term $g_i = (2S_i + 1)(2L_i + 1)$. We have $g_{\mathrm{H}} = 2$ for hydrogen and $g_{\mathrm{O}} = 9$ for oxygen. The statistical weight of diatomic molecules with a zero projection of the total moment is $g_i = (2S_i + 1)$. Thus, $g_{\mathrm{H_2}} = 1$ and $g_{\mathrm{O_2}} = 3$. The states of diatomic molecules with a nonzero projection of the total moment are doubly degenerate $g_i = 2(2S_i+1)$. Therefore, $g_{\mathrm{OH}} = 4$. According to the Jang–Teller theorem (see [28]), the main state of the symmetric triatomic nonlinear molecule is not degenerate; hence, $g_{\mathrm{H_2O}} = 1$.

The statistical sum is decomposed into two parts, rotational and vibrational ones:

$$Z_i(T) = Z_i^r(T) Z_i^v(T).$$

The rotational component of the statistical sum (see [19]) for asymmetric diatomic molecules (OH) is

$$Z_i^r(T) = 2IT/\hbar^2,$$

where I is the moment of inertia of the molecule. For symmetric diatomic molecules (H_2 and O_2), the statistical sum is twice as small:

$$Z_i^r(T) = IT/\hbar^2.$$

For molecules with three different main moments of inertia (I_1, I_2, and I_3), the rotational component of the statistical sum is (see [19])

$$Z_i^r(T) = (2T)^{3/2}\sqrt{\pi I_1 I_2 I_3}/(f\hbar^3).$$

The number of symmetry f for the water molecule equals 2.

The vibrational component of the statistical sum for diatomic molecules for low temperatures ($T < 1$ eV, for which anharmonicity of vibrations can be neglected) is

$$Z_i^v(T) = 1/(1 - \exp(-\hbar\omega/T)),$$

where $\hbar\omega$ is the energy of the quantum of molecular vibrations. In practice, this formula is valid for all temperatures, since the majority of molecules become dissociated at temperatures above 1 eV, and the contribution of the vibrational component of the statistical sum becomes negligible. The H_2O molecule can simultaneously have three orthogonal vibrational motions:

$$Z_{\mathrm{H_2O}}^v(T) = \frac{1}{1 - \exp(-\hbar\omega_1/T)} \frac{1}{1 - \exp(-\hbar\omega_2/T)} \frac{1}{1 - \exp(-\hbar\omega_3/T)}.$$

After substitution of statistical weights and all components of the statistical sum into (12), we obtain the system of equations determining the values of $p_i(T, P)$:

$$\frac{p_{\mathrm{H}}^2}{p_{\mathrm{H_2}}} = 8.13 \cdot 10^6 \Big(1 - \exp\Big(-\frac{0.502}{T}\Big)\Big) \frac{T^{3/2}}{P} \exp\Big(-\frac{4.48}{T}\Big),$$

$$\frac{p_{\mathrm{O}}^2}{p_{\mathrm{O}_2}} = 8.23\cdot 10^7 \Big(1-\exp\Big(-\frac{0.191}{T}\Big)\Big)\frac{T^{3/2}}{P}\exp\Big(-\frac{5.12}{T}\Big),$$

$$\frac{p_{\mathrm{O}}p_{\mathrm{H}}}{p_{\mathrm{OH}}} = 3.67\cdot 10^6 \Big(1-\exp\Big(-\frac{0.433}{T}\Big)\Big)\frac{T^{3/2}}{P}\exp\Big(-\frac{4.4}{T}\Big), \tag{13}$$

$$\frac{p_{\mathrm{H}}p_{\mathrm{OH}}}{p_{\mathrm{H_2O}}} = 1.14\cdot 10^8\,\frac{(1-\exp(-0.198/T))(1-\exp(-0.456/T))(1-\exp(-0.466/T))}{(1-\exp(-0.433/T))}\frac{T^2}{P}\exp\Big(-\frac{5.17}{T}\Big),$$

$$p_{\mathrm{H_2O}} + p_{\mathrm{H_2}} + p_{\mathrm{O_2}} + p_{\mathrm{OH}} + p_{\mathrm{H}} + p_{\mathrm{O}} = 1,$$

$$4p_{\mathrm{O_2}} + p_{\mathrm{OH}} + 2p_{\mathrm{O}} = 2p_{\mathrm{H_2}} + p_{\mathrm{H}}.$$

The potentials of dissociation and energy of vibrational quanta are taken from [27]. The results of calculations by formulas (13) are in good agreement with the data of [26].

Based on the calculated values of p_i, we determine the heat capacity of the vapor mixture. It equals the sum of heat capacities of the species in the mixture:

$$C = N\sum_i c_i p_i.$$

Here N is the total number of particles, p_iN is the number of particles of the ith species, and c_i is the heat capacity of the molecule or atom of the ith species. For instance, the heat capacity of the water molecule is determined by formula (8). The number of particles N changes in the course of dissociation. We introduce a parameter that remains unchanged during dissociation: the number of oxygen nuclei

$$N_{\mathrm{O}} = N(p_{\mathrm{H_2O}} + p_{\mathrm{OH}} + p_{\mathrm{O}} + 2p_{\mathrm{O_2}}),$$

which coincides with the number of water molecules in the case of complete recombination of the vapor mixture, and the relative concentrations

$$\nu_i = \frac{p_iN}{N_{\mathrm{O}}} = \frac{p_i}{p_{\mathrm{H_2O}} + p_{\mathrm{OH}} + p_{\mathrm{O}} + 2p_{\mathrm{O_2}}}.$$

Then, the heat capacity can be written as

$$C = N_{\mathrm{O}}\sum_i c_i\nu_i.$$

4. Allowance for Dissociation During Bubble Compression. Chemical equilibrium during the entire process of compression implies that the rate of variation of vapor parameters is slower than the rate of chemical reactions. Satisfaction of this condition was verified by the chemical reaction of dissociation of water molecules, which is the determining one at the initial stage of dissociation of the vapor mixture. Based on the data of [29], we calculated the dissociation rate K_d of water molecules in the course of the bubble collapse. The compression process itself was considered by formulas (9) without allowance for dissociation. The results of this calculation are plotted in Fig. 4 in comparison with logarithmic derivatives of the vapor parameters.

Up to a temperature of 5000 K, the dissociation rate is much lower than the characteristic rate of the collapse. Hence, there is practically no dissociation below this temperature. In a chemically equilibrium process, dissociation becomes significant already at a temperature of 2500 K. This means that the kinetic approach should be used for calculating dissociation. We introduce the chemical equilibrium parameter $\gamma = \alpha/(1-\nu_{\mathrm{H_2O}})$ (α is the dissociation coefficient). In the case of chemical equilibrium, $\gamma = 1$. To describe the process of compression, we accept the following simplified model: the number of dissociated water molecules αN_{O} is calculated kinetically from the dissociation rate K_d, and then the vapor composition is found by multiplying the chemically equilibrium value by γ. The calculations should also take into account the recombination rate. As in decomposition, the main role in formation of water molecules belongs to binary collisions, e.g., the reaction $\mathrm{OH} + \mathrm{H_2} \to \mathrm{H} + \mathrm{H_2O}$. Therefore, the recombination rate is quadratic with respect to γ; hence, the rate of the decrease in the amount of water is $(1-\gamma^2)K_d$. Because the rate of other reactions leading to equilibrium is either the same as that of water dissociation (e.g., $\mathrm{OH} + \mathrm{H_2O} \to \mathrm{O} + \mathrm{H} + \mathrm{H_2O}$) or higher (the rate of the reaction $\mathrm{H} + \mathrm{H} + \mathrm{H_2O} \to \mathrm{H_2} + \mathrm{H_2O}$ is much higher that

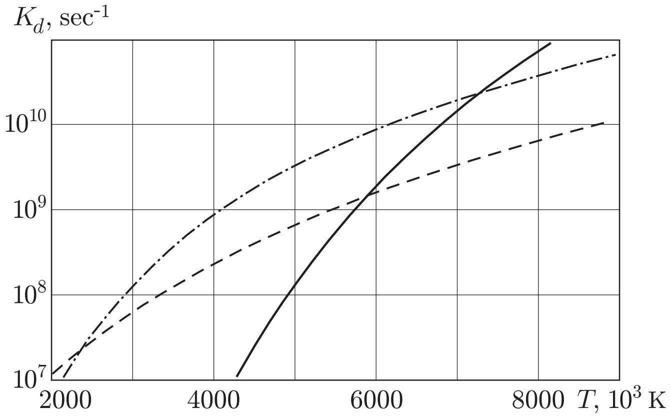

Fig. 4. Rate of variation of vapor parameters in the course of the bubble collapse without allowance for dissociation for the initial parameters $R_0 = 0.5$ mm, $T_0 = 30°$C, and $P_w = 10$ bar: rate of dissociation K_d of water molecules (solid curve), density growth rate $\rho^{-1}\,d\rho/dt$ (dot-and-dashed curve), and temperature growth rate $T^{-1}\,dT/dt$ (dashed curve).

the rate of water dissociation for commensurable concentrations of hydrogen and water), such a simplified approach yields good agreement with the exact kinetic calculation.

With allowance for the model accepted, the internal energy of the molecular gas is $E_{H_2O} - \alpha u$, where $u = E_{H_2O} - \sum_i \nu_i \dfrac{E_i}{1 - \nu_{H_2O}}$ (summation is performed over all components of the vapor mixture). Here, the energy E_i include the potential of molecular dissociation. For instance, the energy of water is determined by the formula $E_{H_2O} = \int c_{H_2O}\,dT - D_{H\text{–}OH} - D_{OH}$. With allowance for dissociation, Eq. (6) should be rewritten as

$$d(E_{H_2O} - \alpha u)N_O = E_{H_2O}\,dN_O - P\,dV. \tag{14}$$

The value of α is determined by the kinetic equation

$$\frac{d\alpha}{(1-\alpha)\,dt} = (1-\gamma^2)K_d.$$

Using (14) instead of (6), we obtain a new system of equations similar to (9) but much more cumbersome.

Allowance for dissociation has practically no effect on the bubble-compression dynamics. This effect is significant only at the final stage. Its influence on the mass exchange between the vapor and the water surface is also weak. Thus, allowance for dissociation alters the final mass of vapor by less than 1%. A significant effect is produced by dissociation on temperature and pressure inside the bubble.

5. Condition of Shock-Wave Emergence. After transition to the gaseous mode of compression, the density of the compressed vapor can reach high values. For further calculations, as the equation of state, we use the two-parameter Redlich–Kwong equation

$$P = \frac{N_A T}{V_\mu - b} - \frac{a}{\sqrt{T}\,V_\mu(V_\mu + b)}, \tag{15}$$

where N_A is the Avogadro number, V_μ is the molar volume, and a and b are the Redlich–Kwong parameters. During the bubble collapse, a decrease in volume is accompanied by an increase in temperature. An analysis shows that the second term of Eq. (15) can be neglected for such a process. The parameter b has the meaning of the volume occupied by electron shells of one mole of particles and, obviously, remains unchanged in the course of dissociation with an unchanged number of nuclei. Taking into account this fact, we write the equation of state in the form

$$PV = \frac{\nu N_O T}{1 - \beta N_O/V}, \tag{16}$$

where $\beta = b/N_A = 2.43 \cdot 10^{-23}$ cm^3 and $\nu = \sum_i \nu_i$. Formula (16) is correct up to the concentration of oxygen nuclei equal to the concentration of water molecules in the liquid state $3.3 \cdot 10^{22}$ cm^{-3}. At high concentrations, P formally tends to infinity, and another equation of state should be used in this case.

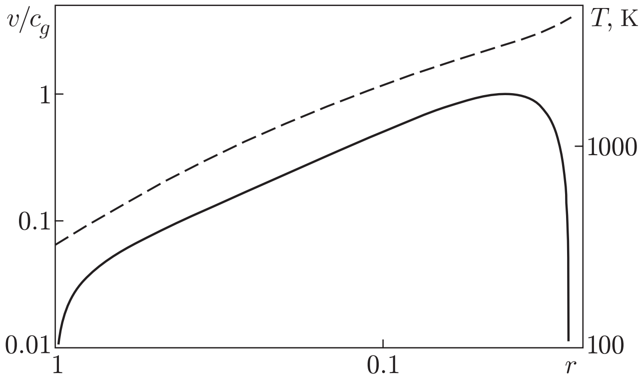

Fig. 5. Dynamics of variation of vapor parameters in the course of the bubble collapse for $R_0 = 3$ mm, $T_0 = 323.16$ K, and $P_w^* = 5.2$ bar: the solid and dashed curves refer to the ratio of the interface velocity to the velocity of sound inside the bubble and to the temperature inside the bubble, respectively.

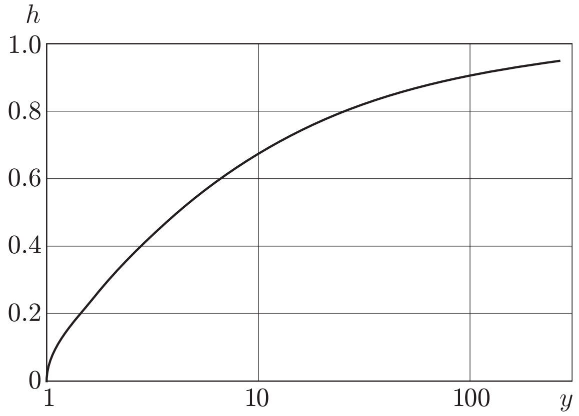

Fig. 6. Function $h(y)$ of the boundary of shock-wave emergence.

To analyze the sufficient conditions of shock-wave emergence, we use the Herring–Gilmore equation (5). The calculations show that the distributions of density and pressure in the bubble are close to uniform before shock-wave origination. For instance, it is shown [7] that, in the case of shock-wave formation, the dynamics of bubble-radius variation almost coincides with the calculation performed by Eq. (5) for a uniform distribution of pressure. Hence, in what follows, we calculate the conditions of shock-wave emergence, assuming that the pressure is uniform.

The shock wave originates as the velocity of the bubble boundary $v = \dot{R}$ exceeds the velocity of sound in the gas c_g. For each initial pressure P_0 and initial radius R_0, we determine the minimum pressure P_w^* for which this condition is satisfied. Calculating the velocity of the bubble boundary by Eq. (5), we choose P_w^* so that the ratio v/c_g in the maximum reaches unity, which is illustrated in Fig. 5. Such a situation mainly occurs owing to the nonlinear effect of density in the equation of state (16). Hence, the density at this point weakly depends on the initial parameters and reaches 0.1–0.2 g/cm^3. Processing of the results of such a calculation reveals the dependence

$$P_w^* = 100 P_0^{3/4} h(y), \tag{17}$$

where $y = 36 R_0 P_0^2$, and the dependence $h(y)$ is plotted in Fig. 6. For water pressures higher than P_w^*, the ratio v/c_g in the course of compression becomes higher than unity, which leads to shock-wave generation. As is seen from Fig. 6, for

$$R_0 < 1/(36 P_0)$$

the shock wave formally emerges for all $P_w > P_0$. Indeed, even a small excess of P_w over P_0 triggers compression. In the case of such slow compression, the temperature on the bubble surface increases weakly, and hence, the pressure inside the bubble remains unchanged and compression continues. If the collapse condition (11) $R_0 < R_*$ is satisfied thereby, the bubble simply collapses; for $R_0 > R_*$, a shock wave is formed. Thus, for small R_0, the condition of shock-wave formation $P_w > P_0$ should be combined with the condition

$$P_w > \Big(\frac{0.0334}{R_0^{0.7} P_0}\Big)^4.$$

For instance, for the initial radius $R_0 = 2$ mm and initial temperature 20°C ($P_0 = 0.0234$ bar), the necessary condition for shock-wave generation in the bubble is $P_w > 0.6$ bar.

After determining the conditions of shock-wave emergence, it becomes possible to determine the maximum reachable temperature under uniform compression. According to (10), for fixed P_w and P_0, the final energy of vapor molecules increases with decreasing R_0. Hence, Eq. (17) determines the surface of parameters for which the maximum temperature under uniform compression is reached. If we fix the value of T_0 and move along the curve $h(y)$ (see Fig. 6) from low to high values, changing P_w and R_0, we find that the energy E rapidly increases first, and then (for $y > 2$) its growth becomes slower, and the energy approaches a certain maximum value. This maximum value turned out to be weakly dependent on T_0 and approximately equal to $6 \cdot 10^4$ K. The integral heat capacity of the water molecule (E/T) at high temperatures approaches 6. Hence, without allowance for dissociation, the maximum temperature is 10^4 K (dissociation at high P_w and R_0 is low). For the initial data of the calculation illustrated in Fig. 5, the energy of one molecule is $3.6 \cdot 10^4$ K ($y = 1.65$); therefore, the temperature, with allowance for integral heat capacity, is $6 \cdot 10^3$ K, which is slightly higher than the result of the dynamic calculation (see Fig. 5) that takes into account dissociation as well.

In the case of shock-wave formation, the temperature can be much higher, but its determination requires a special study.

Conclusions. Vapor condensation in the course of compression of a vapor bubble is responsible for a significant decrease in the amount of the heated substance. Such a decrease can lead to the complete collapse of the bubble. The collapse condition is determined by the initial parameters. A shock wave emerges in a wide range of initial parameters. In this case, it is possible to reach high (above 10^4 K) temperatures. The condition for shock-wave origination is set by a functional dependence of initial parameters of the bubble. In the case of uniform compression, the maximum reachable temperature of vapor is 10^4 K.

Considerable condensation decreases the amount of vapor in the bubble by several orders. This effect can be used for concentration of the substance added to water in the heating zone.

REFERENCES

1. B. P. Barber, C. C. Wu, R. Lofstedt, et al., "Sensitivity of sonoluminescence to experimental parameters," *Phys. Rev. Lett.*, **72**, 1380–1383 (1994).
2. D. F. Gaitan, L. A. Crum, R. A. Roy, and C. C. Church, "Sonoluminescence and bubble dynamics for a single, stable cavitation bubble," *J. Acoust. Soc. Amer.*, **91**, No. 6, 3166–3172 (1992).
3. R. A. Hiller, S. J. Putterman, and K. R. Weninger, "Time-resolved spectra of sonoluminescence," *Phys. Rev. Lett.*, **80**, 1090–1093 (1998).
4. L. A. Crum, "Sonoluminescence, sonochemistry, and sonophysics," *J. Acoust. Soc. Amer.*, **95**, No. 1, 559–562 (1994).
5. W. C. Moss, D. B. Clarke, J. W. White, and D. A. Young, "Hydrodynamic simulation of bubble collapse and picosecond sonoluminescence," *Phys. Fluids*, **6**, No. 9, 2979–2985 (1994).
6. R. I. Nigmatulin, I. Sh. Akhatov, and N. K. Vakhitova, "Forced oscillations of a gas bubble in a spherical volume of a compressible liquid," *J. Appl. Mech. Tech. Phys.*, **40**, No. 2, 285–291 (1999).
7. A. A. Aganin and M. A. Il'gamov, "Numerical simulation of gas dynamics in a bubble during its collapse with the formation of shock waves," *J. Appl. Mech. Tech. Phys.*, **40**, No. 2, 276–284 (1999).
8. R. P. Taleyarkhan, C. D. West, J. S. Cho, et al., "Evidence for nuclear emissions during acoustic cavitation," *Science*, **295**, 1868–1873 (2002).
9. H. Hertz, "Uber die verdunstung der flussigkeiten, inbesondere des quecksilbers, im iufteren raume," *Ann. Phys.*, **17**, 177–190 (1882).
10. M. Knudsen, "Maximum rate of vaporization of mercury," *Ann. Phys.*, **47**, 697–705 (1915).

11. N. A. Gumerov, Ch.-Ts. Hsiao, and A. G. Goumilevski, “Determination of the accommodation coefficient using vapor/gas bubble dynamics in an acoustic field,” Technical Report 98001, NASA/CR-2001-210572 (2001). Available at http://gltrs.grc.nasa.gov/gltrs.
12. I. Akhatov, O. Lindau, A. Topolnikov, and N. Vakhitova, “Collapse and rebound of a laser-induced cavitation bubble,” *Phys. Fluids*, **13**, No. 10, 2805–2819 (2001).
13. S. E. Schwartz, “Historical perspective on heterogeneous gas-particle interaction,” in: *Proc. Mass Accommodation Workshop*, Billerica (2002). Available at http://www.ecd.bnl.gov/steve/ .
14. A. A. Vasil’ev, V. K. Kedrinskii, and S. P. Taratuta, “Dynamics of a single bubble with a chemically active gas,” *Combust. Expl. Shock Waves*, **34**, No. 2, 226–229 (1998).
15. V. K. Kedrinskii, P. A. Fomin, and S. P. Taratuta, “Dynamics of a single bubble in a liquid in the presence of chemical reactions and interphase heat and mass exchange,” *J. Appl. Mech. Tech. Phys.*, **40**, No. 2, 292–299 (1999).
16. Yu. A. Nikolaev and P. A. Fomin, “Approximate equation if kinetics in heterogeneous systems of the gas-condensed-phase type,” *Combust. Expl. Shock Waves*, **19**, No. 6, 737–745 (1983).
17. Yu. A. Nikolaev and D. V. Zak, “Agreement of models of chemical reactions in gases with the second law of thermodynamics,” *Combust. Expl. Shock Waves*, **24**, No. 4, 461–463 (1988).
18. P. A. Fomin and A. V. Trotsyuk, “An approximate calculation of the isentrope of a gas in chemical equilibrium,” *Combust. Expl. Shock Waves*, **31**, No. 4, 455–458 (1995).
19. L. D. Landau and E. M. Lifshits, *Statistical Physics*, Pergamon Press (1980).
20. H. R. Pruppacher and J. D. Klett, *Microphysics of Clouds and Precipitation: Second Revised and Enlarged Edition with an Introduction to Cloud Chemistry and Cloud Electricity*, Kluwer Acad. Publ., Dordrecht (1996).
21. K. S. Hickman, “Maximum evaporation coefficient of water,” *Chem. Eng. Sci.*, **18**, 1442–1451 (1954).
22. A. F. Mills and R. A. Seban, “The condensation coefficient of water,” *Int. J. Heat Mass Transfer*, **37**, 1815–1827 (1967).
23. U. Narasawa and G. S. Springer, “Measurements of evaporation rates of water,” *J. Coll. Int. Sci.*, **50**, 392–395 (1975).
24. S. S. Kutateladze and V. E. Nakoryakov, *Heat and Mass Transfer and Waves in Gas–Liquid Systems* [in Russian], Nauka, Novosibirsk (1984).
25. R. T. Knapp, J. W. Daily, and F. G. Hammitt, *Cavitation*, McGraw-Hill, New York (1970).
26. N. B. Vargaftik, *Handbook on Thermophysical Properties of Gases and Liquids* [in Russian], Nauka, Moscow (1972).
27. A. A. Ravdel’ and A. M. Ponomareva, *Brief Handbook on Chemistry* [in Russian], Khimiya, Leningrad (1983).
28. L. D. Landau and E. M. LIfshits, *Quantum Mechanics. Nonrelativistic Theory* [in Russian], Nauka, Moscow (1974).
29. V. N. Kondrat’ev, *Rate Constants of Gas-Phase Reactions: Handbook* [in Russian], Nauka, Moscow (1971).